Int. J. Heat Mass Transfer. Vol. 35, No. 11, pp. 2891–2903, 1992
Printed in Great Britain

0017-9310/92 $5.00+0.00

Heat transfer performance comparisons of five different rectangular channels with parallel angled ribs

J. S. PARK, J. C. HAN, Y. HUANG and S. OU
Turbine Heat Transfer Laboratory, Department of Mechanical Engineering, Texas A & M University, College Station, TX 77843, U.S.A.

and

R. J. BOYLE
Heat Transfer Fundamentals Section, NASA Lewis Research Center, Cleveland, OH 44135, U.S.A.

(*Received* 6 *August* 1991 *and in final form* 11 *December* 1991)

Abstract—This paper systematically presents the results of heat transfer and friction factor data measured in five short rectangular channels with turbulence promoters. The project investigated the combined effects of the channel aspect ratio, rib angle-of-attack, and flow Reynolds number on heat transfer and pressure drop in rectangular channels with two opposite ribbed walls. The channel aspect ratio (width-to-height, W/H, ribs on side W) varied from 1/4 to 1/2, to 1, 2, and 4, while the corresponding rib angles-of-attack α were 90°, 60°, 45°, and 30°, respectively. The Reynolds number range was 10,000–60,000. The results suggest that the narrow aspect ratio channels ($W/H < 1$) give much better heat transfer performance than the wide aspect ratio channels ($W/H > 1$). For the square channel ($W/H = 1$), the 60°/45° angled ribs provide the best heat transfer performance. For the narrow aspect ratio channel ($W/H = 1/4$ or $1/2$), the 45°/60° angled ribs are recommended while the 30°/45° angled ribs are better for wide aspect ratio channels ($W/H = 4$ or 2).

INTRODUCTION

It is common for turbulence promoters/vortex generators such as fins, pins, ribs, twisted tapes, inserts, etc., to be widely used in heat exchangers to improve the single-phase heat transfer performance [1]. This paper belongs in the category of surface heat transfer augmentation by the use of repeated-rib turbulence promoters. Heat transfer enhancement has been studied [2–8] for fully developed turbulent flows in circular tubes and between parallel plates with repeated-rib promoters. Studies also exist for these ribbed surfaces with high temperature gas-cooled nuclear reactor applications [9–12]. In recent years, however, the major motivation for research has been for high temperature gas turbine cooling systems [13–18], as in the present investigation.

The improvement in power and efficiency of modern aircraft gas turbine engines has led to increased maximum turbine inlet temperatures (1400–1500°C). As a consequence, developing various cooling technologies for vanes and blades of advanced gas turbines becomes more important in industry. In advanced gas turbine vanes and blades, repeated-rib turbulence promoters are cast onto two opposite walls of internal cooling passages to enhance heat transfer to the cooling air since heat is conducted from the pressure and suction surfaces. The internal cooling passages can be modeled as short rectangular channels with different aspect ratios. Due to blade shape, cooling channels near the trailing edge have broad aspect ratios ($W/H \geqslant 1$) and those near the leading edge have narrow aspect ratios ($W/H < 1$) as in Fig. 1. The heat transfer performance depends on the channel aspect ratio, the rib configuration (such as rib height, pitch, angle-of-attack), and the flow Reynolds number. Reference [19] studied the effects of rib configurations ($0.046 \leqslant e/D \leqslant 0.078$, $10 \leqslant P/e \leqslant 20$, $30° \leqslant \alpha \leqslant 90°$) and flow Reynolds numbers ($10{,}000 \leqslant Re \leqslant 60{,}000$) on the local heat transfer and pressure drop in developing (entrance) and fully developed regions of foil heated, short rectangular channels ($10 \leqslant L/D \leqslant 15$) with wide aspect ratios ($W/H = 1$, 2, and 4). Reference [20] reported similar studies in rectangular channels of narrow aspect ratios ($W/H = 1/4$ and $1/2$). Some data reported in refs. [19, 20] have been published in refs. [21, 22]. These publications [21, 22] focused on the local heat transfer coefficient distributions, average heat transfer coefficient and friction factor, and their correlations. However, the combined effects of channel aspect ratio and rib angle-of-attack on the heat transfer performance were not clearly presented. For example, it has been concluded that the 30° angled rib in the square channel has the best thermal performance per given pumping power and the 60° angled rib has the highest heat transfer and pressure drop per given Reynolds number. It is not clear whether this finding

NOMENCLATURE

A	heat transfer surface area
D	channel hydraulic diameter
e	rib height
f	friction factor in a channel with two opposite ribbed walls
f_0	friction factor in a developed four-sided smooth channel
g_c	conversion factor
G	mass flux, ρv
h	local heat transfer coefficient
H	flow channel height
K	thermal conductivity of air
L	test channel length for frictional pressure drop
Nu	Nusselt number, hD/K
Nu_0	Nusselt number in a fully developed four-sided smooth channel
p	pressure in channel
p_{atm}	atmosphere pressure
P	rib pitch
Pr	Prandtl number of air
ΔP	pressure drop across the test section
q	heat generation rate from foils
q_{loss}	heat loss rate through insulation
Re	Reynolds number, GD/μ
T_b	bulk mean temperature of air
T_w	local wall temperature
v	average velocity of air.

Greek symbols

α	rib angle-of-attack
μ	average dynamic viscosity of air
ρ	average density of air.

is applicable to rectangular channels with wider or narrower aspect ratios. On the other hand, for a given angled rib configuration, it is not clear whether the wider or narrower aspect ratio channel will provide a better heat transfer performance. It is necessary to present the combined effects of channel aspect ratio and rib angle on the heat transfer performance.

This paper is based on original data presented in two reports [19, 20]. The objective is to compare the heat transfer performance in five rectangular channels with parallel, angled ribs. The channel aspect ratios (W/H, ribs on side W) are 1/4, 1/2, 1, 2, and 4, as seen in Fig. 1. The channel length-to-hydraulic diameter ratios (L/D) are 10 and 15. The ribs are placed parallel on the two opposite walls in each channel with a rib angle 90°, 60°, 45°, or 30° to the flow, respectively. This means the ribs on the top surface are parallel to the ribs on the bottom surface and to each other. The rib height-to-hydraulic diameter ratios (e/D) are 0.047 and 0.078 and the rib pitch-to-height ratio (P/e) is 10. These e/D and P/e ratios are typical in turbine cooling channels. The flow Reynolds numbers are 10,000, 30,000, and 60,000 for a given rectangular channel so the obtained results are of heat transfer vs pressure drop for four rib angles. The results of heat transfer vs pressure drop are compared for a given rib angle for five rectangular channels. The highest and lowest heat transfer coefficient accompanied by the highest/lowest pressure drop are identified in each of five rectangular channels with angled ribs. Although the main application of this study is for internal cooling passages of gas turbine blades and vanes, the results can be used for heat exchangers with rectangular cross-sectional channels and with repeated-rib turbulence promoters. All raw data in this study are documented in two reports [19, 20]. Additional information related to this paper may be found in refs. [21, 22].

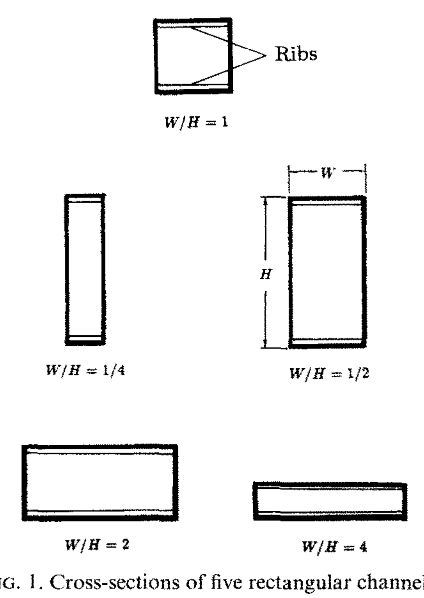

FIG. 1. Cross-sections of five rectangular channels.

EXPERIMENTAL APPARATUS AND DATA REDUCTION

The experimental program used in the study was described in some detail in refs. [21, 22]. A brief introduction is presented here to clarify the configuration parameters that relate to the present study.

A sketch of the experimental apparatus is shown in Fig. 2. Five straight rectangular channels with different aspect ratios were constructed. A plenum connected to the inlet of the test channel provided a sudden entrance condition (hydrodynamically developing flow). The air was exhaused into the atmosphere after the test channel. In order to obtain the local heat

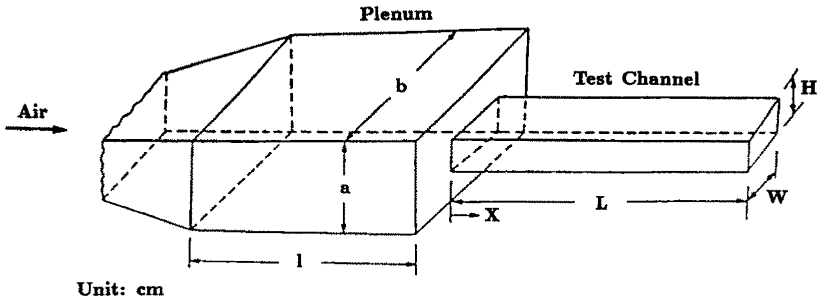

	W	H	W/H	D	L	b	a	CR	l
Square Channel	5.1	5.1	1	5.1	127.5	15.3	15.3	9	15D
Rectangular Channel I	10.2	5.1	2	6.8	127.5	30.6	15.3	9	15D
Rectangular Channel II	10.2	2.55	4	4.08	127.4	30.6	15.3	18	25D
Rectangular Channel IA	5.1	10.2	2/4	6.8	127.5	30.6	15.3	9	15D
Rectangular Channel IIA	2.55	10.2	1/4	4.08	127.5	30.6	15.3	18	25D

FIG. 2. Dimensions of the test channels and the inlet plenum.

transfer coefficients, the test channels were uniformly heated by passing a current through 0.025 mm (0.001 in.) thick, stainless steel foils cemented separately to the inner face of four plates, which composed the channel. Figure 2 shows the dimensions of the test channels and the associated plenums. These parameters were arbitrarily chosen to simulate typical turbine cooling channels. The flow Reynolds number based on the channel hydraulic diameter (D) varied between 10,000 and 60,000.

The brass ribs with a square cross-section were uniformly glued on the top and bottom walls of the foil heated test channels so that the ribs on the opposite walls (side W) were parallel. Figure 3 shows the rib geometries for each test channel. The glue thickness is less than 0.0127 cm. The rectangular channel IA ($W/H = 1/2$) and the rectangular channel IIA ($W/H = 1/4$) were fabricated from the rectangular channel I ($W/H = 2$) and rectangular channel II ($W/H = 4$), respectively, by simply moving ribs from the top and bottom walls to the right- and left-hand side walls of the channels. The entire heated test channel was insulated by fiberglass material.

For local surface temperature measurements, 180 36-gauge copper–constantan thermocouples were soldered underneath the foils in the square channel and rectangular channels I and II (100 in the rectangular channels IA and IIA), respectively. Ninety of these thermocouples were placed on the bottom ribbed wall (channel width side); the other 90 on the right-hand side smooth wall (channel height side). Sixty of the 90 thermocouples were placed along the centerline of the ribbed and the smooth walls, as shown in Fig. 4. The remaining 30 were distributed on the middleline and the edgeline of each wall. The thermocouples were soldered underneath the thin foil through holes in the wood–plexiglass plate, as shown in Fig. 4. The thermocouple locations were fixed, although the rib angle α varied from 90° to 30°. Six pressure taps along the centerline of the top wall and six along the centerline of the left-hand side wall measured static pressure drop. Another pressure tap installed at the plenum recorded the static pressure of entering air. Thermocouple and pressure tap locations for each test channel are given in refs. [21, 22].

The local heat transfer coefficient was calculated from the local net heat transfer rate per unit surface area to the cooling air, the local wall temperature on each foil plate, and the local bulk mean air temperature as:

$$h = (q - q_{\text{loss}})/[A(T_w - T_b)]. \tag{1}$$

Equation (1) was used for the local ribbed side wall and smooth side wall heat transfer coefficient calculations. The local net heat transfer rate was the electrical power generated from the foil heaters minus the heat loss outside the test duct. The electrical power generated from the foil was determined from the measured foil resistance and voltage on each wall of the test duct. The effect of the local wall temperature variation on the local foil resistance was estimated to be very small and negligible. The foil provided a nearly uniform heat flux on each wall of the test duct. The heat loss from the test duct was determined separately under a no flow condition. The maximum heat loss from the ribbed side wall and smooth side wall was estimated to be less than 3 and 5%, respectively, for Reynolds numbers greater than 10,000.

Note that the ribbed side wall heat transfer surface area increases by adding ribs. The area increment

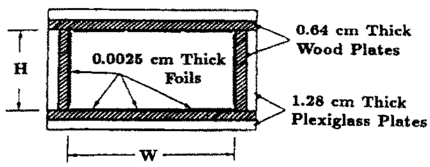

(a)

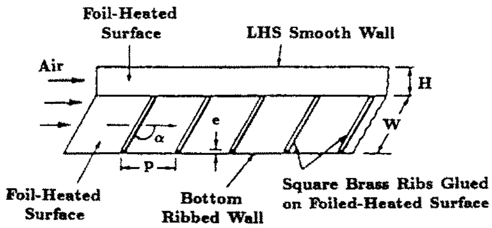

(b)

	W/H	e	e/D	P/e	α	Re*10^{-3}
Square Channel	1	0.24	0.047	10	90°,60° 45°,30°	10 30 60
Rectangular Channel I	2	0.32	0.047	10	90°,60° 45°,30°	10 30 60
Rectangular Channel II	4	0.32	0.078	10	90°,60° 45°,30°	10 30 60
Rectangular Channel IA	2/4	0.32	0.047	10	90°,60° 45°,30°	10 30 60
Rectangular Channel IIA	1/4	0.32	0.078	10	90°,60° 45°	10 30 60

FIG. 3. (a) Cross-section of foil heated test channel. (b) Rib geometries in each test channel.

depends upon the rib spacing and rib angle-of-attack. For the present study of $P/e = 10$, the ribbed side wall heat transfer area with the 90° ribs increases by 20% compared with the smooth wall, while the heat transfer area with the 60° ribs increases by 23%. To place the results on a common basis, the heat transfer area used in equation (1) was always that of a smooth wall. The local wall temperatures used in equation (1) were read from the thermocouple output of each foil plate. The bulk mean air temperatures entering and leaving the test duct were measured by thermocouples. The local bulk mean air temperature used in equation (1) was calculated from the measured inlet air temperature and the net heat input to the air. The total net heat transfer rate from the test duct to the cooling air agreed with the cooling air enthalpy rise along the test duct. The inlet bulk mean air temperature was 24–30°C depending on the test conditions. The maximum uncertainty in the Nusselt number was estimated to be less than 8% for Reynolds numbers larger than 10,000 by using the uncertainty estimation method of Kline and McClintock [23].

To reduce the influence of flow Reynolds number on the heat transfer augmentation, the local Nusselt number of the present study was normalized by the Nusselt number for fully developed turbulent flow in smooth circular tubes correlated by Dittus–Boelter and McAdams as:

$$Nu/Nu_0 = (hD/K)/[0.023Re^{0.8}Pr^{0.4}]. \qquad (2)$$

A micromanometer connected to pressure taps measures the pressure drop across the test duct. The friction factor was calculated from the pressure drop across the test duct and the mass velocity of air as:

$$f = \Delta P/[4(L/D)(G^2/2\rho g_c)]. \qquad (3)$$

Based on the heating levels of this study, it was experimentally determined that the friction factor with heating is about 1–3% higher than that without heating. Therefore, the friction factor f is based on the isothermal conditions (tests without heating). The maximum uncertainty in the friction factor is estimated to be less than 9% for Reynolds numbers greater than 10,000 by using the uncertainty estima-

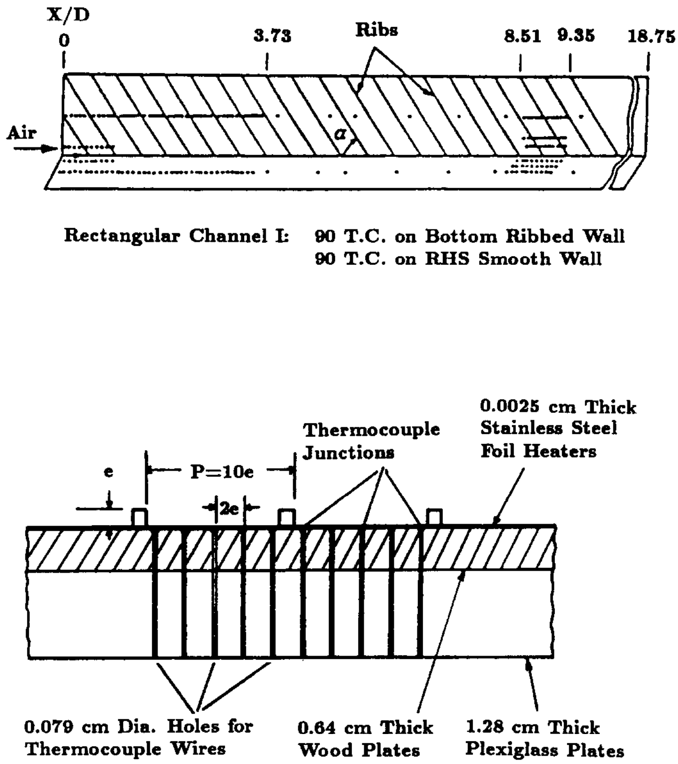

FIG. 4. Detailed thermocouple locations in each test channel.

tion method of Kline and McClintock [23]. To reduce the effect of flow Reynolds number on the friction factor increment, the friction factor f of the present study was normalized by the friction factor for fully developed turbulent flow in smooth circular tubes ($10^4 < Re < 10^6$) proposed by Blasius as:

$$f/f_0 = f/[0.046Re^{-0.2}]. \quad (4)$$

For effective turbine cooling design, it is important to know the local heat transfer distributions for developing flow in short rectangular channels with rib turbulators. Therefore, during the experiment, raw data such as the local temperature were acquired point by point along the centerlines of the ribbed side and smooth side walls. These kind of results provide the detailed distributions of heat transfer coefficient on channel walls from the entrance to the downstream region [21, 22]. However, it is inconvenient to apply in the design of turbine airfoil cooling channels.

For the results of ribbed channels to be useful for designers, and to express the characteristics of heat transfer with rib turbulators, an average evaluation of the data on those points between the ribs is taken based on the Cubic Spline Function Integration. That is, each established Nusselt number is based on the average evaluation of the data on five stations every rib pitch (pitch-average) along the axial line for the case of $P/e = 10$ (see Fig. 4). After evaluation, the effect of important parameters such as the channel aspect ratio, rib angle-of-attack, and the Reynolds number on the augmentation of heat transfer will be shown more concisely. From a mathematical view, the Cubic Spline Function Integration used in this study has the same accuracy as the Simpson Integration and is easier to apply than the latter. It would meet the requirement of engineering design.

EXPERIMENTAL RESULTS AND DISCUSSION

Comparison between the present and previous investigations

Typical results for the four-sided smooth square channel are shown in Fig. 5(a). The test data from refs. [24, 25] are included for comparison. In ref. [24], the data were obtained for air flow in a circular tube with a sharp entrance and heated by condensing steam. In ref. [25], the results were based on air flow in a high-aspect-ratio rectangular channel ($W/H = 18$) with a sharp entrance by using the naphthalene sublimation method. In general, the local Nusselt number ratios along the bottom wall (channel width side) and the right-hand-side wall of the test channel exhibit the same trend. This shows that flow separation occurs right after the entrance due to sharp contractions with flow reattachment attained at about $0.5D$ from the entrance, creating a high heat transfer coefficient. In

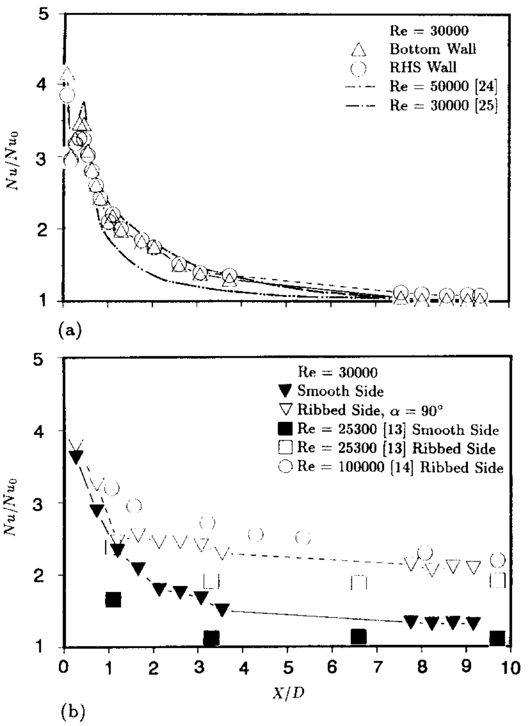

FIG. 5. (a) The local Nusselt number ratio in the four-sided smooth square channel. (b) The local Nusselt number ratio in the two-sided ribbed square channel.

the entrance region, the present data agree qualitatively with those of refs. [24, 25]. In the downstream region with $X/D > 8$, the present data agree fairly well with those of refs. [24, 25] and are about 5–10% higher than Dittus–Boelter–McAdams' fully developed turbulent tube flow results. Note that both the present data and ref. [25] show that the flow reattachment (the highest heat transfer) is attained at about $0.5D$ from the sharp entrance.

Typical results for the two-sided ribbed square channel (with 90° ribs) are shown in Fig. 5(b). The pitch-averaged heat transfers are presented as the axial distributions of a normalized Nusselt number ratio, Nu/Nu_0, as given in equation (2). The test data of 90° ribs from refs. [13, 14] are included for comparison. In ref. [13], the data were obtained for air flow in two-sided ribbed square duct with a short duct sharp entrance and heated by copper-plate heaters. In ref. [14], the results were based on the air flow in a two-sided ribbed square duct with a 90° bend sharp entrance and heated by thin foil heaters. The ribs break up the laminar sublayer and create local wall turbulence due to flow separation from the ribs and reattachment between the ribs. Therefore, the ribbed-side wall heat transfer coefficients are much higher than the smooth-side wall heat transfer coefficients, except that in the entrance region both side heat transfer coefficients are comparable. Due to the ribbed-side wall turbulence, the smooth-side wall heat transfer coefficients in the downstream region are also higher than the four-sided smooth channel results. Note that in the upstream region the present data are slightly lower than those in ref. [14], and higher than those in ref. [13], but agree fairly well with each other in the downstream region. In the entrance region, the different heat transfer coefficients between this study and those of refs. [13, 14] are due to the fact that different types of sharp entrances were used in each investigation. In the downstream region the agreeable heat transfer coefficients among these studies are because the flows become fully developed in the same type of rib-roughened channels. These smooth and ribbed channel results prove that the test sections and instrumentations of this study are reliable to reproduce data for various rib configurations and flow channel aspect ratios.

The average heat transfer coefficient and the average friction factor in the fully developed region of the four-sided smooth rectangular channels are shown in Fig. 6 and compared with the existing correlations for flow in fully developed turbulent tube flow. The Nusselt numbers differ by up to 10% from the Dittus–Boelter–McAdams equation, and the friction factors differ by up to 12% from the Blasius equation.

Pitch-averaged heat transfer and pressure drop data

Several results were obtained by the above method for 60 sets of combinations (five W/H ratios, four rib angles, and three Reynolds numbers). The pitch-averaged heat transfer results are presented as the axial (streamwise) distributions of a normalized Nusselt number ratio, Nu/Nu_0, as given in equation (2). The results plotted in Fig. 7 show the combined effects

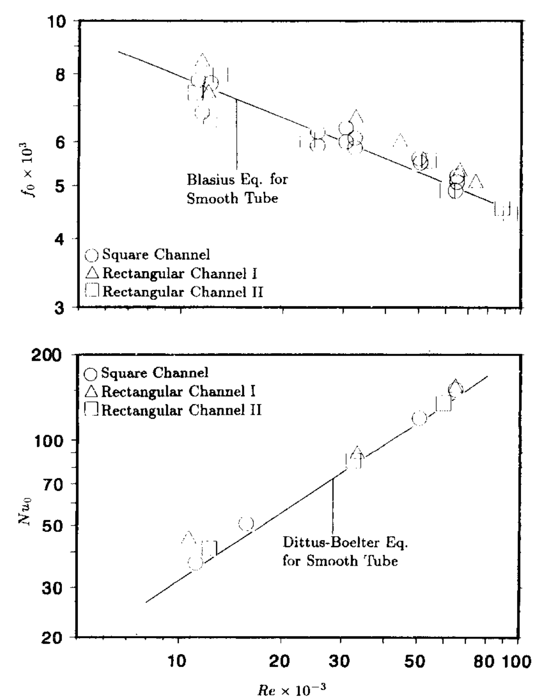

FIG. 6. The fully developed friction factor and Nusselt number in the four-sided smooth rectangular channel.

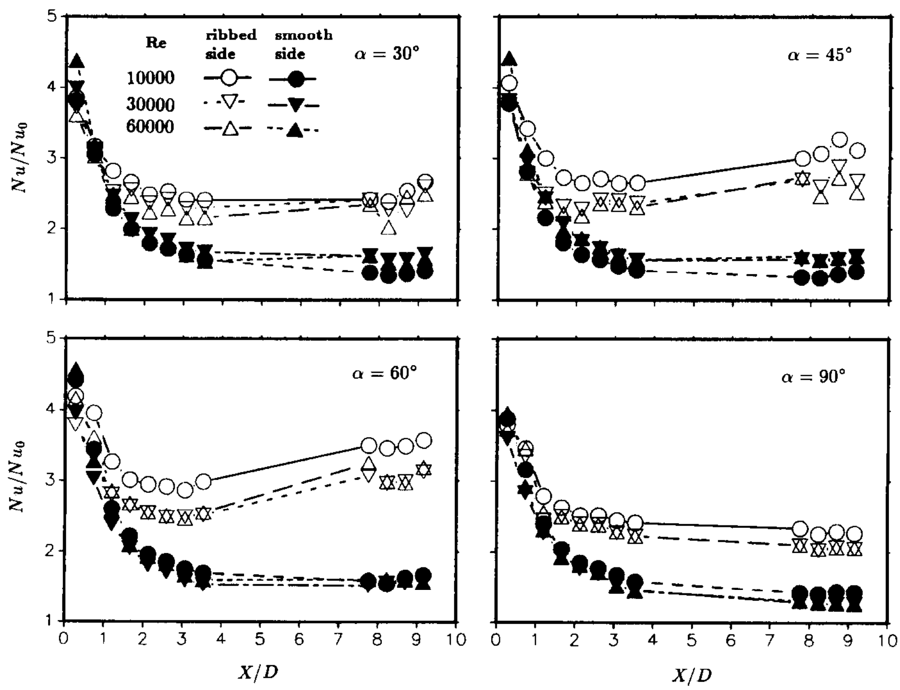

FIG. 7. The effect of rib angle on the pitch-averaged heat transfer distribution in the square channel ($W/H = 1$).

of the channel aspect ratio, rib angle-of-attack, and the Reynolds number on the centerline Nusselt number ratios for the square channel ($W/H = 1$). From entrance to developing flow, which corresponds to $X/D = 0$–1.5 on the ribbed side and 2.5 on the smooth side, heat transfer first decreases sharply then stays constant, except that heat transfer increases after $X/D \geqslant 3$ for $\alpha = 45°$ and $60°$. The Nusselt number ratios at the ribbed sides in the cases of $\alpha = 30°$ and $90°$ are lower than those for $\alpha = 45°$ and $60°$. The secondary flow induced by rib angle/orientation causes higher heat transfer for $\alpha = 45°$ and $60°$. Although heat transfer ratio decreases slightly with increasing Reynolds number, the results of $Re = 10{,}000$ in the cases of $\alpha = 45°$ and $60°$ are higher than the others. Reference [20] shows similar plots for $W/H = 1/2$, $1/4$, 2, and 4.

The heat transfer augmentation in rib-roughened channels is always accompanied by an increased pressure drop through the same channels. In order to comprehensively evaluate heat transfer and flow characters in a channel, a set of local pressure drop distributions corresponding to different Reynolds numbers and rib angles-of-attack for the square channel ($W/H = 1$) are shown in Fig. 8. The local friction factor was defined as $(p - p_{atm})/(1/2\rho v^2)$ for comparison with equation (3). A first data point at $X < 0$ means that it was in the plenum. It is clear that, for all Reynolds numbers studied, the local dimensionless pressure drop at $\alpha = 60°$ is the highest among those at other rib angles at $\alpha = 45°$, $90°$, and $30°$, and also for the four-sided smooth channel. The dimensionless pressure drop increases slightly as the Reynolds number increases. Similar kinds of plots of $W/H = 1/2$, $1/4$, 2, and 4 are shown in ref. [20].

As discussed in refs. [21, 22], the parallel angled ribs may induce secondary flow (or swirling flow) along the rib axes. Therefore, the Nusselt number ratios on both the smooth-side wall and the ribbed-side wall with parallel angled ribs ($\alpha = 60°$, $45°$) are higher than that with transverse ribs ($\alpha = 90°$). Because of this secondary flow effect, the pressure drops with parallel angled ribs ($\alpha = 60°$ and $45°$) are also higher than the 90° ribs. This rib-angle-induced secondary flow effect is significant for flow in a square channel and in a rectangular channel with narrow aspect ratio ($W/H = 1/2$). However, this effect is gradually reduced for the rectangular channels with broad aspect ratos ($W/H = 2$ and 4), as discussed in refs. [21, 22]. This may be because the secondary flows induced by parallel angled ribs on the two opposite walls cancel each other out, because the two opposite walls are too close to each other for broad aspect ratio channels ($W/H = 2$ and 4). The conjectured secondary flow induced by the angled ribs will be verified through the flow visualization technique and by velocity profile measurements in a separate project. This investigation focuses on the effect of channel aspect ratio on the surface heat transfer enhancement with the angled ribs.

Centerline-averaged heat transfer and pressure drop data

Based on the pitch-averaged Nusselt number ratio and the dimensionless pressure drop distribution, it was found that for $\alpha = 90°$, the pitch-averaged Nusselt

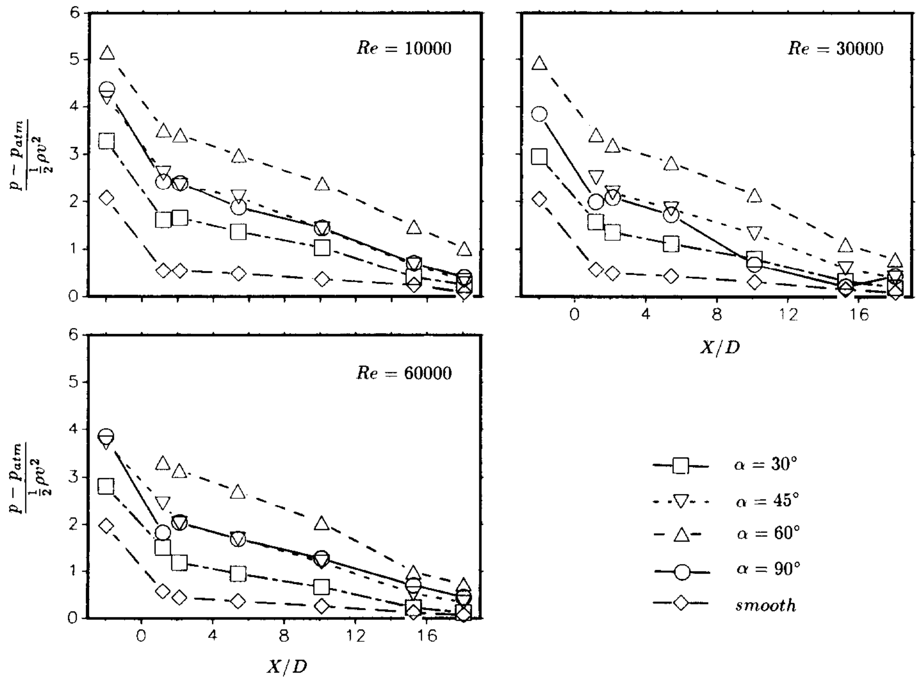

FIG. 8. The effect of rib angle on the pressure drop distribution in the square channel ($W/H = 1$).

number ratio and the friction factor became fully developed constant values after $X/D > 2$. Therefore, the heat transfer and pressure drop data in the region with $X/D > 2$ in each channel were used to provide the centerline-averaged Nusselt number and the friction factor. The heat transfer coefficients along the centerline after $X/D \geqslant 2$ were averaged separately for the ribbed-side and smooth-side walls. Figure 9 provides a comparison of the centerline-averaged Nusselt number ratios versus Reynolds number for different channel aspect ratios. As seen in Fig. 9, the centerline-averaged heat transfer ratios for the rectangular channels decrease slightly with increasing Reynolds numbers on both the ribbed-side and smooth-side walls. Figure 9 shows that for all channels studied, the normalized Nusselt number on the ribbed-side wall at $\alpha = 60°$ is the highest and, in turn, at $\alpha = 45°$ and $30°$; whereas $\alpha = 90°$ is the lowest except for the rectangular channels I and II ($W/H = 2$ and 4), where $\alpha = 90°$ provides the highest heat transfer. As indicated above, this is because the rib-angle-induced secondary flow is significant in narrow aspect ratio channels ($W/H = 1/4$, $1/2$, and 1) and causes higher heat transfer. However, the secondary flow effect diminishes in broad aspect ratio channels ($W/H = 2$ and 4); therefore, the 90° rib produces higher heat transfer. For the smooth-side wall, the average heat transfer at $\alpha = 90°$ in the rectangular channels I and II ($W/H = 2$ and 4) is so high that they are close to those at $\alpha = 30°$ on the ribbed-side wall.

Figure 10 is the average friction factor calculated by equation (4) after $X/D \geqslant 2$. As expected, the average friction factor ratios increase with increasing Reynolds number. The average friction factor ratios for broad aspect ratio channels ($W/H > 1$) depend on the rib angle, but they are insensitive to the rib angle for narrow aspect ratio channels ($W/H < 1$). The average friction factor ratios increase with increasing rib angle (i.e. 90° ribs produce the highest friction factor ratios) for $W/H = 2$ and 4, while the 60° angled ribs provide the highest friction factor ratios for $W/H = 1$, $1/2$, and $1/4$. In general, the average friction factor ratios increase with increasing channel aspect ratio from $1/4$ to 4.

Heat transfer performance comparison

A simple method to evaluate the heat transfer performance for rib-roughened channels is the comparison of both heat transfer and friction factor augmentations, as shown in Figs. 11 and 12. In these figures, for a given rib angle in a given channel, the Nusselt number ratios decrease but the friction factor ratios increase with increasing Reynolds number from 10,000 to 60,000.

As indicated in Fig. 11 for the square channel ($W/H = 1$), the ribbed-side heat transfer enhancements are about three times and the pressure drop penalties are about four to eight times the values for 60°/45° ribs. For the same level of heat transfer enhancement ($\sim$three-fold) for the narrow aspect ratio channels ($W/H = 1/2$ and $1/4$), the pressure drop penalties are only twice to four times the values for 60°/45° ribs. However, for the same level of heat transfer enhancement for the broad aspect ratio channel ($W/H = 4$), the pressure drop penalties are as high as 8–16 times the values for 60°/45° ribs. It can be

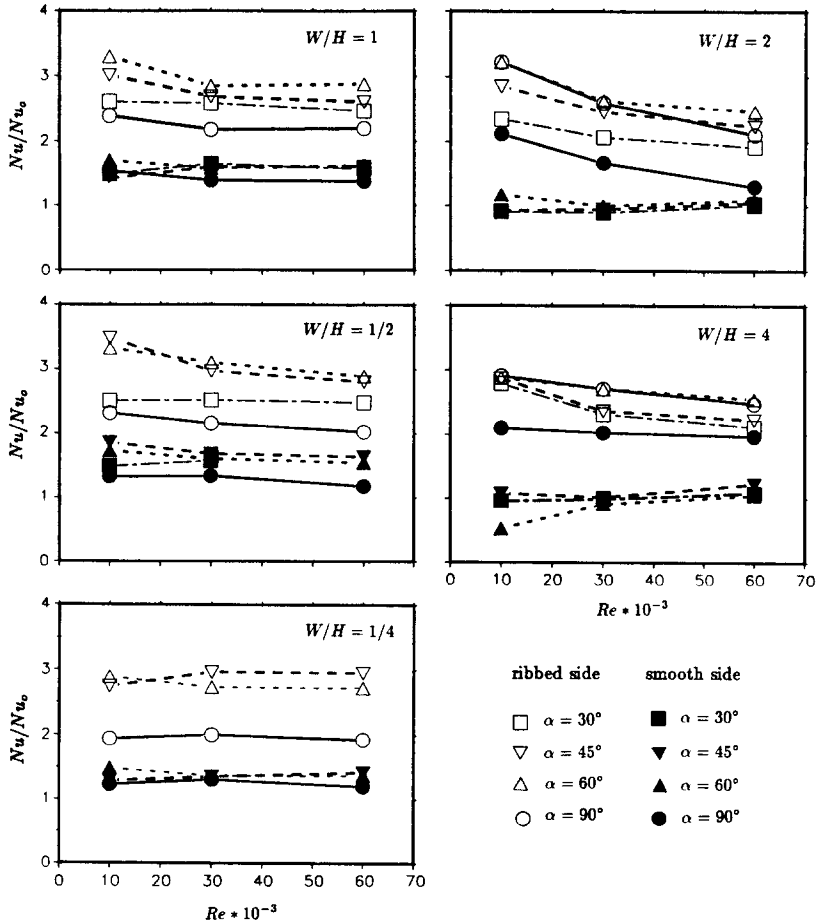

FIG. 9. Average heat transfer vs Reynolds number—effect of channel aspect ratio.

concluded that the narrow aspect ratio channel does better than the broad aspect ratio channel. Figure 11 also shows that the 90° ribs give the lowest heat transfer and pressure drop augmentations, whereas the 60° ribs provide the highest heat transfer and pressure drop enhancements for $W/H = 1/2$ and $1/4$; the 30° ribs give the lowest while the 90° ribs provide the highest heat transfer and pressure drop augmentations for $W/H = 4$ and 2.

Figure 12 shows the effect of channel aspect ratio on the heat transfer and pressure drop enhancement for a given rib angle at three Reynolds numbers. For 60° ribs, the ribbed-side heat transfer augmentations are almost constant (~three-fold) but the pressure drop penalties increase dramatically from two- to 18-fold when the channel aspect ratio changes from 1/4 to 4. Similar results are observed for 45° ribs. It is clear that the narrow aspect ratio channel provides a better heat transfer performance than the broad aspect ratio channel. Both heat transfer enhancement (two- to three-fold) and pressure drop increment (two- to seven-fold) are relatively low for 30° ribs in all five channels ($W/H = 1/4$–4). The heat transfer is enhanced 2–2.5-fold and pressure drop two- to five-fold for 90° ribs at $W/H = 1/4$–1, but the heat transfer is enhanced three-fold and pressure drop 12–18-fold for 90° ribs at $W/H = 4$.

From an application point of view, one would like to use the 60° or 45° angled ribs in a square channel ($W/H = 1$) because they enhance the heat transfer coefficient about three times and pay four to eight times the pressure drop for Reynolds numbers between 10,000 and 60,000. If one has a choice, the narrow aspect ratio channel ($W/H = 1/2$ and $1/4$) with 45°/60° angled ribs will be the best because it creates about three times the heat transfer coefficient but only pays three to four times the pressure drop for the same range of Reynolds numbers. This is because the spacing between the two opposite ribbed walls is bigger for the narrow aspect ratio channel. In the narrow aspect ratio channel the angled rib secondary flow effect still exists (and causes high heat transfer) but the pressure drop is greatly reduced when compared with the square channel. Two options exist if one has no choice and must use the broad aspect ratio channel ($W/H = 4$). First, use 90° ribs to enhance the heat transfer coefficient three times and pay a 12–18-fold drop in pressure; second, use 30° ribs to enhance the heat transfer coefficient two- to three-fold and only pay a six-fold pressure drop. Both

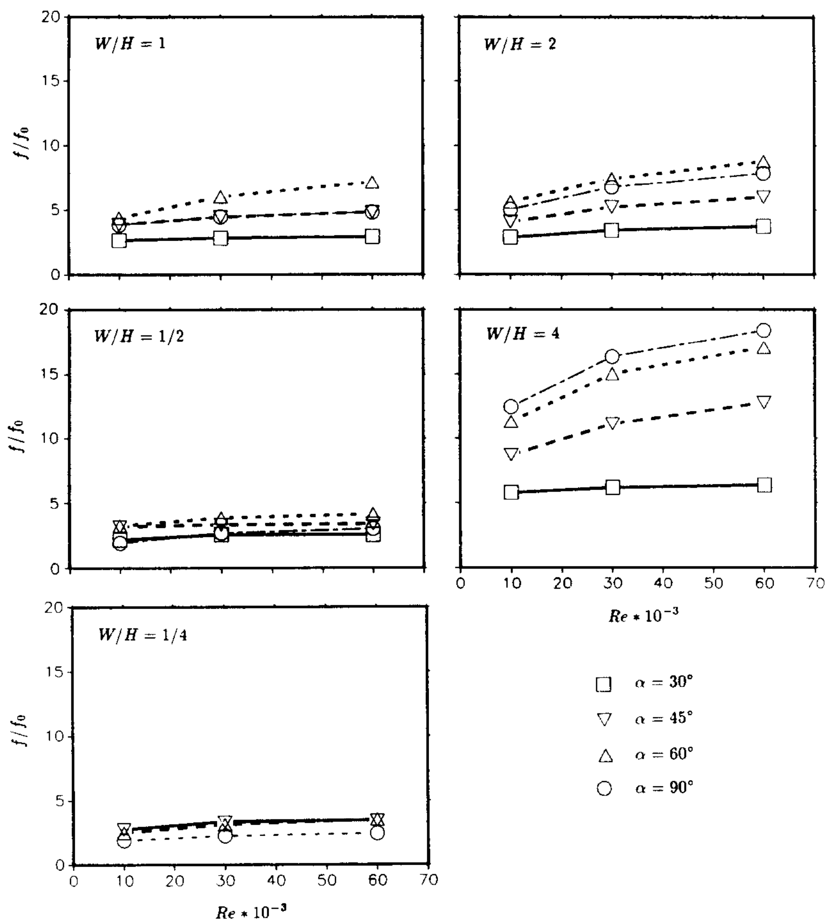

FIG. 10. Average friction factor vs Reynolds number—effect of channel aspect ratio.

the heat transfer enhancement and pressure drop penalty for the broad aspect ratio channel with 60°/45° angled ribs are somewhere between those of the 90° and 30° ribs.

CONCLUDING REMARKS

The effect of channel aspect ratio on the heat transfer performance in five different rectangular channels with angled ribs has been systematically investigated.

1. The slope of Nu/Nu_0 vs f/f_0 decreases with increasing W/H ratio from 1/4 to 4. This means the pressure drop increments in the broad aspect ratio channel ($W/H = 4$) are much larger than in the narrow aspect ratio channel ($W/H = 1/4$) for the same level of heat transfer augmentation.

2. For $W/H = 1$, 1/2, and 1/4, the order of heat transfer and pressure drop augmentation is 60°, 45°, and 30°/90° angled ribs. For $W/H = 4$ and 2, the augmentation order is 90°/60°, 45°, and 30° angled ribs.

3. For $W/H = 1/2$ and 1/4, the 45°/60° angled ribs have about three-fold heat transfer augmentation with about three- to four-fold pressure drop penalty. For $W/H = 1$, the 60°/45° angled ribs give about a three-fold heat transfer augmentation with a four- to eight-fold pressure drop penalty. However, for the same level of heat transfer augmentation, the pressure drop increments are about 8–16 times greater for $W/H = 4$.

4. For narrow aspect ratio channels ($W/H = 1/4$ and 1/2), the 45°/60° angled ribs are recommended for cooling design ($Nu/Nu_0 = 3$–3.5, $f/f_0 = 4$). For the broad aspect ratio channel ($W/H = 4$), the 30°/45° angled ribs are recommended for cooling design ($Nu/Nu_0 = 2$–3, $f/f_0 = 4$–6).

5. For 60° angled ribs, the heat transfer augmentations are about three-fold for all five channels studied. However, the pressure drop penalties increase from four- to 18-fold when the channel aspects ratio changes from 1/4 to 4. For 45° angled ribs, both heat transfer and pressure drop increments are slightly lower than the 60° angled ribs in the corresponding channels. For 30° angled ribs, both heat transfer (two- to three-fold) and pressure drop increment (two- to seven-fold) are relatively low in all five channels. For 90° ribs, the heat transfer is enhanced 2–2.5-fold and pressure drop two- to five-fold at $W/H = 1/4$–1, but the heat transfer is enhanced three-fold and pressure drop 12–18-fold at $W/H = 4$.

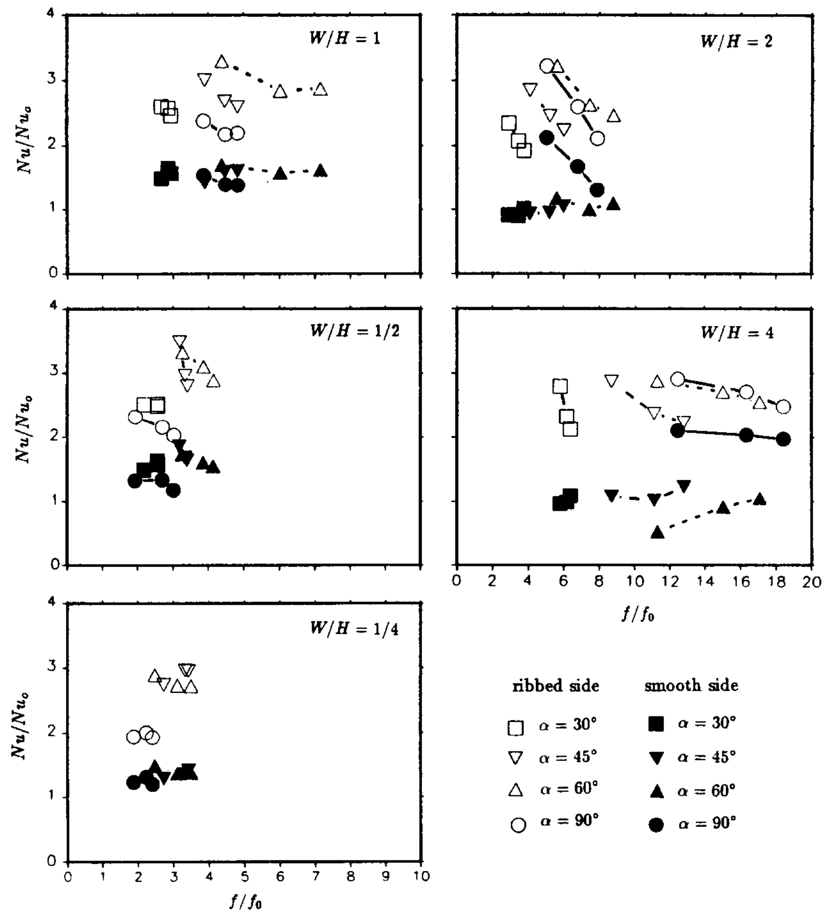

FIG. 11. Comparison of heat transfer performance—effect of rib angle.

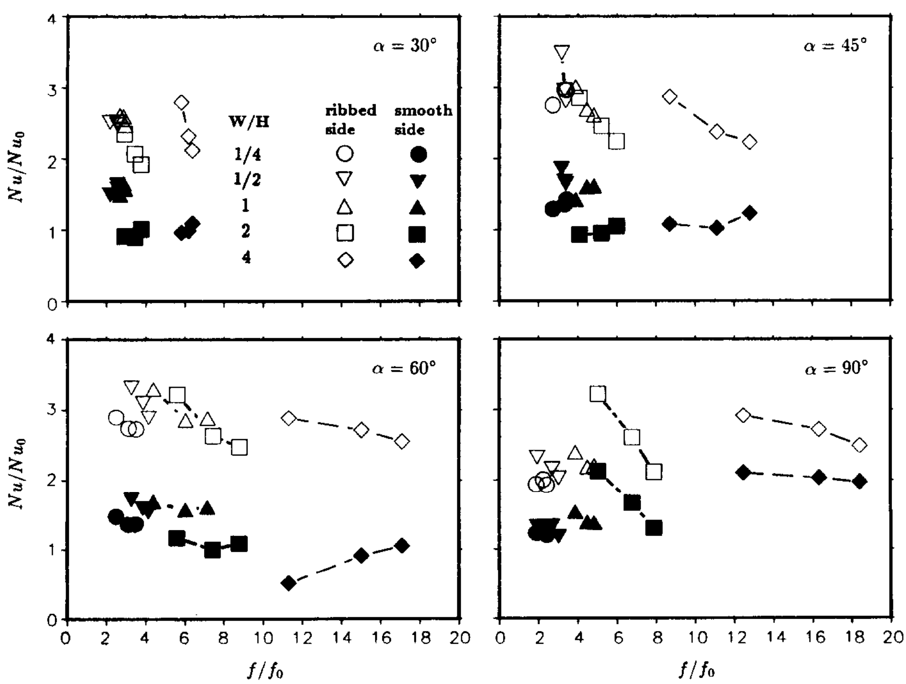

FIG. 12. Comparison of heat transfer performance—effect of channel aspect ratio.

Acknowledgements—This work was funded by the NASA-Lewis Research Center under grant No. NAG 3-311 and contract No. NAS 3-24227. Very special thanks are due to Dr Robert Simoneau of the NASA-Lewis Research Center for supporting the project. The support of Mr Curtis Walker (deceased 1985) of the U.S. Army Propulsion Laboratory as well as the efforts of Mr Francis Stepka (deceased 1982) of the NASA-Lewis Research Center were invaluable to this project. This concluding report is dedicated to their memory.

REFERENCES

1. A. E. Bergles and R. L. Webb, Bibliography on augmentation of convective heat and mass transfer. In *Augmentation of Convective Heat and Mass Transfer* (Edited by A. E. Bergles and R. L. Webb), pp. 1–15. ASME, New York (1970).
2. R. H. Norris, Some simple approximate heat transfer correlations for turbulent flow in ducts with rough surfaces. In *Augmentation of Convective Heat and Mass Transfer* (Edited by A. E. Bergles and R. L. Webb), pp. 16–26. ASME, New York (1970).
3. R. L. Webb, E. R. G. Eckert and R. J. Goldstein, Heat transfer and friction in tubes with repeated-rib roughness, *Int. J. Heat Mass Transfer* **14,** 601–617 (1971).
4. M. J. Lewis, An elementary analysis for predicting the momentum and heat transfer characteristics of a hydraulically rough surface, *ASME J. Heat Transfer* **97,** 249–254 (1975).
5. B. A. Kader and A. M. Yaglom, Turbulent heat and mass transfer from a wall with parallel roughness ridges, *Int. J. Heat Mass Transfer* **20,** 354–357 (1977).
6. J. C. Han, L. R. Glicksman and W. M. Rohsenow, An investigation of heat transfer and friction for rib-roughened surfaces, *Int. J. Heat Mass Transfer* **21,** 1143–1156 (1978).
7. D. L. Gee and R. L. Webb, Forced convective heat transfer in helically rib-roughened tubes, *Int. J. Heat Mass Transfer* **23,** 1127–1136 (1980).
8. R. Sethumadhaven and M. Raja Rao, Turbulent flow heat transfer and fluid friction in helical-wire-coil-inserted tubes, *Int. J. Heat Mass Transfer* **26,** 1833–1844 (1983).
9. W. B. Hall, Heat transfer in channels having rough and smooth surfaces, *J. Mech. Engng Sci.* **4,** 287–291 (1962).
10. L. White and D. Wilkie, The heat transfer and pressure loss characteristics of some multi-start ribbed surfaces. In *Augmentation of Convective Heat and Mass Transfer* (Edited by A. E. Bergles and R. L. Webb), pp. 55–62. ASME, New York (1970).
11. M. Dalle Donne and L. Meyer, Turbulent convective heat transfer from rough surfaces with two-dimensional rectangular ribs, *Int. J. Heat Mass Transfer* **20,** 582–620 (1977).
12. L. Meyer, Thermohydraulic characteristics of single rods with three-dimensional roughness, *Int. J. Heat Mass Transfer* **25,** 1043–1058 (1982).
13. F. Burggraf, Experimental heat transfer and pressure drop with two-dimensional turbulence promoter applied to two opposite walls of a square duct. In *Augmentation of Convective Heat and Mass Transfer* (Edited by A. E. Bergles and R. L. Webb), pp. 70–79. ASME, New York (1970).
14. R. J. Boyle, Heat transfer in serpentine passages with turbulence promoters, ASME Paper No. 84-HT-24 (1984).
15. J. C. Han, Heat transfer and friction in channels with two opposite rib-roughened walls, *ASME J. Heat Transfer* **106,** 774–781 (1984).
16. J. C. Han, J. S. Park and C. K. Lei, Heat transfer enhancement in channels with turbulence promoters, *ASME J. Engng Gas Turbines Pwr* **107,** 628–635 (1985).
17. D. E. Metzger and R. P. Vedula, Heat transfer in triangular channels with angled roughness ribs on two walls, *Exp. Heat Transfer* **1,** 31–44 (1987).
18. M. E. Taslim and S. D. Spring, Friction factors and heat transfer coefficients in turbulated cooling passages of different aspect ratios, part I: experimental results, *23rd AIAA/ASME/SAE/ASEE Joint Propulsion Conf.*, San Diego, Paper No. AIAA-87-2009 (1987).
19. J. C. Han, J. S. Park and M. Y. Ibrahim, Measurement of heat transfer and pressure drop in rectangular channels with turbulence promoters, NASA Contractor Report 4015, pp. 1–197 (1986).
20. Y. Huang and J. C. Han, Heat transfer and pressure drop in five straight rectangular channels with parallel angled rib turbulators, Technical Report RF-5037 extended for NASA Contract, Texas A&M University, pp. 1–156 (1990).
21. J. C. Han and J. S. Park, Developing heat transfer in rectangular channels with rib turbulators, *Int. J. Heat Mass Transfer* **31,** 183–195 (1988).
22. J. C. Han, S. Ou, J. S. Park and C. K. Lei, Augmented heat transfer in rectangular channels of narrow aspect ratios with rib turbulators, *Int. J. Heat Mass Transfer* **32,** 1619–1630 (1989).
23. S. J. Kline and F. A. McClintock, Describing uncertainties in single-sample experiments, *Mech. Engng* **75,** 3–8 (1953).
24. L. M. K. Boelter, G. Young and H. W. Iversen, An investigation of aircraft heaters—distribution of heat transfer rate in the entrance section of a circular tube, NACA Technical Note No. 1451 (1948). Data reported by Kays and Crawford in *Convective Heat and Mass Transfer*, 2nd Edn, p. 269. McGraw-Hill, New York (1980).
25. E. M. Sparrow and N. Cur, Turbulent heat transfer in symmetrically or asymmetrically heated flat rectangular duct with flow separation at inlet, *ASME J. Heat Transfer* **104,** 82–89 (1982).

COMPARAISONS DES PERFORMANCES DE TRANSFERT THERMIQUE DE CINQ CANAUX RECTANGULAIRES DIFFERENTS AVEC DES CANELURES PARALLELES OBLIQUES

Résumé—On présente systématiquement les réultats sur le transfert thermique et le coefficient de frottement mesurés pour cinq canaux rectangulaires courts avec des promoteurs de turbulence. On étudie les effets combinés du rapport de forme du canal, de l'angle d'attaque des canelures et du nombre de Reynolds sur le transfert thermique et la perte de pression dans des canaux rectangulaires avec deux parois opposées canelées. Le rapport de forme (largeur/hauteur, W/H, canelure sur le côté W) 1/4, 1/2, 1, 2 et 4 tandis que l'angle d'attaque correspondant α est respectivement 90°, 60°, 45° et 30°. Le domaine du nombre de Reynolds est 10 000–60 000. Les résultats suggèrent que les rapports de forme petits ($W/H < 1$) donnent des meilleures performances de transfert thermique que les grands rapports ($W/H > 1$). Pour le canal carré ($W/H = 1$), les angles 60°/45° donnent les meilleures performances du transfert. Pour les petits rapports de forme ($W/H = 1/4$ ou 1/2), les angles 45°/60° sont recommandés tandis que les angles 30°/45° sont meilleurs pour les grands rapports de forme ($W/H = 4$ ou 2).

VERGLEICH DES WÄRMEÜBERGANGS IN FÜNF UNTERSCHIEDLICHEN RECHTECK-KANÄLEN MIT PARALLEL AUSGERICHTETEN RIPPEN

Zusammenfassung—In der vorliegenden Arbeit werden Ergebnisse für Wärmeübergang und Druckabfall dargestellt, die in fünf kurzen Rechteck-Kanälen mit Turbulenzpromotoren gemessen wurden. Die gekoppelten Einflüsse des Seitenverhältnisses im Kanal, des Anstellwinkels der Rippen sowie der Reynolds-Zahl auf Wärmeübergang und Druckabfall in einem Rechteck-Kanal mit zwei gegenüberliegenden berippten Wänden wird untersucht. Dabei sind die Breitseiten berippt, und das Seitenverhältnis des Kanals (Breite zu Höhe, W/H) beträgt 1/4, 1/2, 1, 2 und 4, während der Anstellwinkel der Rippen, α, die Werte 90°, 60°, 45° und 30° annimmt. Die Reynolds-Zahl liegt im Bereich zwischen 10000 und 60000. Die Ergebnisse deuten darauf hin, daß die Kanäle mit kleinem Seitenverhältnis ($W/H < 1$) ein wesentlich besseres Wärmeübertragungsverhalten aufweisen als die Kanäle mit großem Seitenverhältnis ($W/H > 1$). Bei quadratischem Kanal ($W/H = 1$) ergeben die mit 60°/45° angestellten Rippen das günstigste Wärmeübertragungsverhalten. Für ein kleines Seitenverhältnis ($W/H = 1/4$ oder 1/2) sind die 45°/60° angestellten Rippen zu empfehlen, während für ein großes Verhältnis ($W/H = 4$ oder 2) die 30°/45° angestellten Rippen besser sind.

СРАВНЕНИЕ ХАРАКТЕРИСТИК ТЕПЛОПЕРЕНОСА ПЯТИ РАЗЛИЧНЫХ КАНАЛОВ ПРЯМОУГОЛЬНОГО СЕЧЕНИЯ С ПАРАЛЛЕЛЬНЫМИ РАСПОЛОЖЕННЫМИ ПОД УГЛОМ РЕБРАМИ

Аннотация—Представлены результаты измерений теплопереноса и коэффициента терния в пяти коротких каналах прямоугольного сечения с турбулизаторами. Исследовалось влияние отношения сторон канала, угла атаки ребер и числа Рейнольдса течения на теплоперенос и перепад давления в прямоугольных каналах с двумя оребренными противоположными стенками. Отношение сторон канала (отношение ширины к высоте W/H, при этом ребра расположены на боковых стенках) принимало значения 1/4, 1/2, 1, 2 и 4, а соответствующие углы атаки ребер составляли 90°, 60°, 45° и 30°. Число Рейнольдса изменялось в диапазоне 10000–60000. Полученные результаты свидетельствуют о том, что узкие каналы ($W/H < 1$) обладают гораздо лучшими характеристиками теплопереноса, чем широкие ($W/H > 1$). В случае квадратного канала оптимальные характеристики теплопереноса достигаются при наличии ребер с отношением углов 60°/45°. Для узких каналов ($W/H = 1/4$ или 1/2) рекомендуются угловые ребра с отношением 45°/60°, в то время как для широких каналов ($W/H = 4$ или 2) наиболее эффективны ребра с отношением 30°/45°.